Computers and Concrete, *Vol. 17, No. 2 (2016) 227-240*
DOI: http://dx.doi.org/10.12989/cac.2016.17.2.227

Analytical performance evaluation of modified inclined studs for steel plate concrete wall subjected to cyclic loads

Jin-Sun Lim[1a], Young-Do Jeong[2b], Jin-Won Nam[3c], Chun-Ho Kim[4d] and Seong-Tae Yi[*5]

[1]*Department of Civil Engineering, Inha University, Incheon 22212, Korea*
[2]*R&D Center, POSCO E&C, Incheon 22009, Korea*
[3]*Baytech Korea Inc., 8F, 464 Dunchon-Daero, Jungwon-gu, Seongnam-si, Gyeonggi-do, 13229, Korea*
[4]*Department of Civil Engineering, Joongbu University, Gyeonggi 10279, Korea*
[5]*Department of Civil and Environmental Engineering, Inha Technical College, Incheon 22212, Korea*

(Received October 6, 2015, Revised November 26, 2015, Accepted December 14, 2015)

Abstract. An analytical study was conducted to investigate the effect of the shape and spacing of modified inclined studs used as shear connector between concrete and steel plate on the cyclic behavior of steel plate concrete (SC) shear wall. 9 different analysis cases were adopted to determine the optimized shape and spacing of stud. As the results, the skeleton curves were obtained from the load-displacement hysteresis curves, and the ultimate and yielding strengths were increased as the spacing of studs decrease. In addition, the strength of inclined studs is shown to be bigger compared to that of conventional studs. The damping ratios increased as the decrease of stiffness ratio. Finally, with decreasing the spacing distance of studs, the cumulative dissipated energy was increased and the seismic performance was improved.

Keywords: modified inclined stud, steel plate concrete, shape, spacing, cumulative dissipated energy, seismic performance

1. Introduction

Steel plate concrete (SC) structures is composed of composite body filled with concrete between two steel plates and the steel plates and concrete are connected by studs, which are used as shear connectors. It is generally assumed that, when SC walls are designed and analyzed, steel plates and concrete connected with studs are perfectly bonded for composite behavior.

By using the steel plate on behalf of the reinforcing bar used in the traditional reinforced concrete (RC) structure, the SC structure supplies in-plane and out-of-plane strengths necessary for members and serves the role of formwork; more specifically, the performance as the shear wall is

∗Corresponding author, Professor, E-mail: yist@inhatc.ac.kr
[a]Ph.D., E-mail: coreplay@hanmail.net
[b]Ph.D., E-mail: jdy@poscoenc.com
[c]Ph.D., E-mail: jwnam72@gmail.com
[d]Ph.D., E-mail: chkim@joongbu.ac.kr

Copyright © 2016 Techno-Press, Ltd.
http://www.techno-press.org/?journal=cac&subpage=8 ISSN: 1598-8198 (Print), 1598-818X (Online)

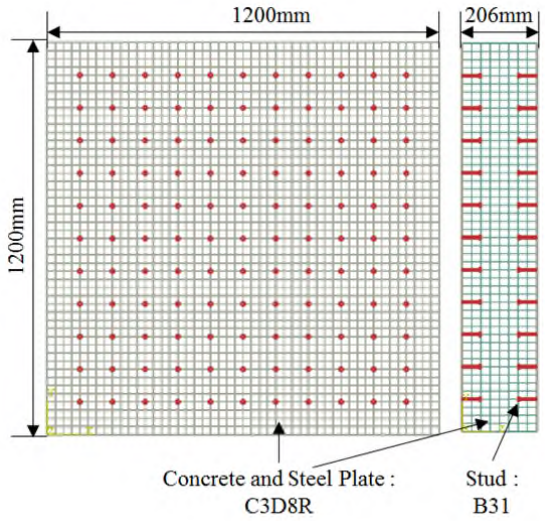

Fig. 1 Finite element model of a SC wall

excellent. The SC member can secure the seismic performance due to the reduction of the cross-section since it is possible to ensure the stiffness similar to the RC using the more thin thickness compared to the cross-section of the RC member. In addition, in terms of functional, it is known that the construction period is relatively quick and the quality management is not difficult compared to RC structures (Cho *et al*. 2013, Lim *et al*. 2014).

But, even today, the researches for SC structures compared to RC or steel structures are relatively not sufficient. Most studies carried out in South Korea and overseas are for the static behavior and, on the dynamic behavior, it was only partially performed. Among them, Ozaki *et al*. (2004) performed the cyclic loading tests for various conditions such as the thickness of steel plate, stud diameter, compressive strength of concrete, axial force, and around opening, etc. for SC shear walls. Lee and Kim (2010) analyzed the results obtained through free vibration tests for the force of low levels than the ultimate strength of the wall and presented the damping ratio. Vecchio and McQuade (2011) performed the analyses on the cyclic load after improving a two-dimensional finite element analysis model. Cho *et al*. (2013) measured the damping ratio over the impact test, when a small-scaled specimen is in the initial stage non-damaged by an external force. In addition, for the same specimen, the variances in the damping ratios through the experiments applied cyclic load were evaluated. Epackachi *et al*. (2014) examined analytically the in-plane shear strength of SC walls and examined the dynamic behavior through the experiments subjected to cyclic load.

This study undertook nonlinear finite element analysis (FEA) to examine the effect of the shape and spacing of the studs on the composite behavior of non-reinforced SC walls subjected to in-plane cyclic loads. In addition, the seismic related criteria and related research results for cyclic loads of KEPIC SNG (KEA 2010) were compared with the analytical results.

2. Finite element analysis of SC shear walls

FEA was conducted to assess the influence of the stud shape and spacing on the composite

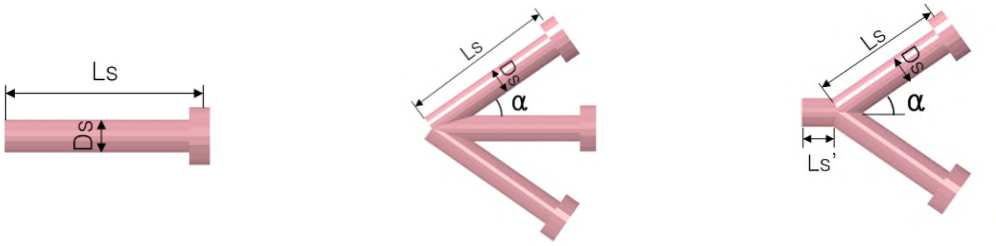

(a) Conventional stud (b) Modified stud #1 (c) Modified stud #2

Fig. 2 Types of stud

behavior of SC shear walls subjected to cyclic load. Finite element (FE) models of SC walls are established with three stud distances and three stud shapes. Additional verification of FE models is omitted in this paper, as the validity of FE models was discussed in a previous study (Cho *et al*. 2014). The ABAQUS/Explicit program was utilized for feasible FEA on the nonlinear behavior of SC walls.

2.1 Shape and element of FE model

For comparison with the results obtained by existing tests, in this study, it is judged that the size of the simple shaped wall specimen used in laboratory tests is more reasonable than the complex shaped real structure. Accordingly, the size of the SC wall model was determined based on the experimental data of Ozaki *et al*. (2004) as follows: 1,200 mm×1,200 mm×206 mm, and 3 mm-thick and 200 mm-thick for the steel plate and concrete, respectively (Fig. 1). In order to obviously observe the effect of studs used as shear connector between concrete and steel plate, the thickness of the steel sheet was determined a thin level than the minimum thickness of KEPIC SNG (KEA 2010) and within the experiment scope of Ozaki *et al*. (2004). Meanwhile, the studies based on numerical analyses using a computer (Ren *et al*. 2015a, b, Shahidul Islam and Khennane 2013) have been a lot done.

In previous researches (Cho *et al*. 2014a, b) performed the static nonlinear analyses, C3D20R

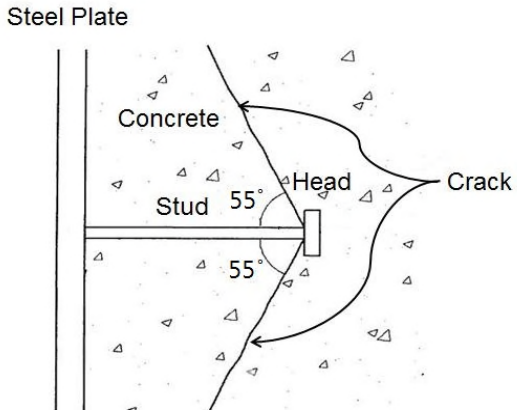

Fig. 3 Localized concrete crack at the stud (ACI 2011)

Table 1 Types and arrangement of studs

Model No.	Arrangement of studs		
	Type	Spacing	Number of specimens
GS-100×100	General stud	100 mm×100 mm	36
GS-167×167	General stud	167 mm×167 mm	16
GS-250×250	General stud	250 mm×250 mm	9
DS1-100×100	Developed stud #1	100 mm×100 mm	108
DS1-167×167	Developed stud #1	167 mm×167 mm	48
DS1-250×250	Developed stud #1	250 mm×250 mm	27
DS2-100×100	Developed stud #2	100 mm×100 mm	72
DS2-167×167	Developed stud #2	167 mm×167 mm	32
DS2-250×250	Developed stud #2	250 mm×250 mm	18

*500 mm×500 mm (area considered in the evaluation)

element was used. However, the element is not supported under the Explicit analysis environments. Accordingly, C3D8R element was used and the mesh was divided to two times more dense compared to previous studies. The relatively small size of the stud allows it to be simply modeled as a beam element (B31). Three stud spacings are considered: 100 mm, 167 mm, and 250 mm. The size of the stud is determined considering the thickness of the concrete, as follows: a diameter of 8mm (stud head diameter: 14 mm), and a length of 50 mm (body 45 mm+head 5 mm). There are three stud shapes used in this study, termed DS1 & DS2 (developed) and GS (general), as in the study of Cho *et al*. (2014a, b) (Fig. 2). The slope (α) of the inclined studs (ACI, 2011, CCD method, Fig. 3) is set to 35° considering the inclination of concrete cracks incurred by the pulling of GS, in which the inclined studs are perpendicular to the crack lines of GS. The stud is assumed to be welded and completely attached to the steel plate. Table 1 explains the shape and spacing of the studs in each analysis model.

2.2 Connection of the members and definition of the contact surface

The direct connection of a beam element to a three-dimensional solid element induces an error in numerical analyses due to the differences in the degrees of freedom. To solve this problem, the structural coupling method in the ABAQUS interaction module is employed to connect a stud to a steel plate. The embedded element method is applied to show the status of the stud embedded in the concrete, which is defined to enable the insert element to transform according to main body's modification when the mother body moves. To analyze the contact behavior between the steel plate and the concrete, a contact method based on an energy method is used and the friction behavior is defined under the assumption of the minor attaching force between concrete and steel plate. The friction coefficient (μ) of the contact surface between the steel and the concrete is assumed to be 0.5.

2.3 Properties of the materials

2.3.1 Concrete

As concrete filled between steel plates shows nonlinear quasi-brittle behavior under tensile and

Table 2 Parameters of the concrete plastic model

Parameters	Input value
Dilation angle	35.0
Eccentricity	0.1
K^*	0.667
Viscosity parameter	0.0
Ratio of the ultimate biaxial compressive stress to the ultimate uniaxial compressive stress	1.12
Ratio of the uniaxial tensile to the uniaxial compressive strength	0.1

*Ratio of second stress invariant on the tensile meridian to that on compression meridian at the initial yield for any given value of the pressure invariant

compressive loadings, in order to express this property, a concrete-damaged-plasticity constitutive model is applied. The uniaxial compressive strength of concrete and the Poisson's ratio used in the analyses, respectively, are assumed to be 35 MPa and 0.18. The modulus of elasticity is set to 29,779 MPa from Eq. (1) considering the Concrete Structure Standard (KCI 2012).

$$E_c = 0.077 m_c^{1.5} \sqrt[3]{f_{cu}} \text{ , MPa} \tag{1}$$

where, f_{cu} is the average compressive strength of concrete (MPa) and m_c is the unit mass (kg/m^3). The values in Table 2 are applied as plasticity parameters of the concrete-damaged-plasticity model based on research by Prakash *et al*. (2011). The compressive stress-strain relationship of concrete is calculated by Eq. (2), as suggested by Carreira and Chu (1985). The tensile stress-strain relationship is determined by the experiment results of Evans and Marathe (1967), while the stress-strain-damage relationship is determined based on researches for cyclic loads by Jankowiak and Łodygowski (2005).

$$\sigma_c = \frac{f_c' \varphi \left(\frac{\varepsilon_c}{\varepsilon_c'} \right)}{\varphi - 1 + \left(\frac{\varepsilon_c}{\varepsilon_c'} \right)^{\varphi}} \text{ , MPa} \tag{2}$$

where, σ_c is the compressive stress of the concrete (MPa), ε_c is the compressive strain, f'_c is the compressive strength, ε'_c is the strain (=0.002) corresponding to the compressive strength, and φ is identical to Eq. (3).

$$\varphi = \left(\frac{f_c'}{32.4} \right) + 1.55 \text{ , MPa} \tag{3}$$

The stress-strain-damage relationship of the concrete is shown in Fig. 4.

2.3.2 Steel plate and stud

As the material characteristics of the steel plate and the stud, the elastic modulus and the Poisson's ratio are set to 207,000 MPa and 0.3, respectively, while the elasto-plastic behavior is

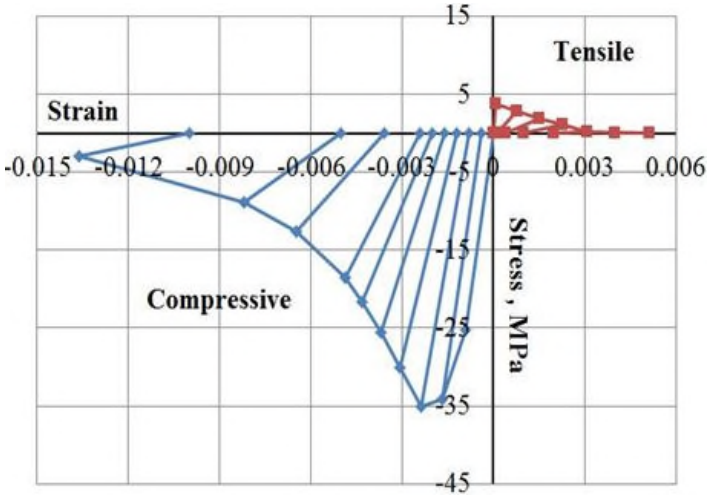

Fig. 4 Stress-strain-damage relationship of the concrete

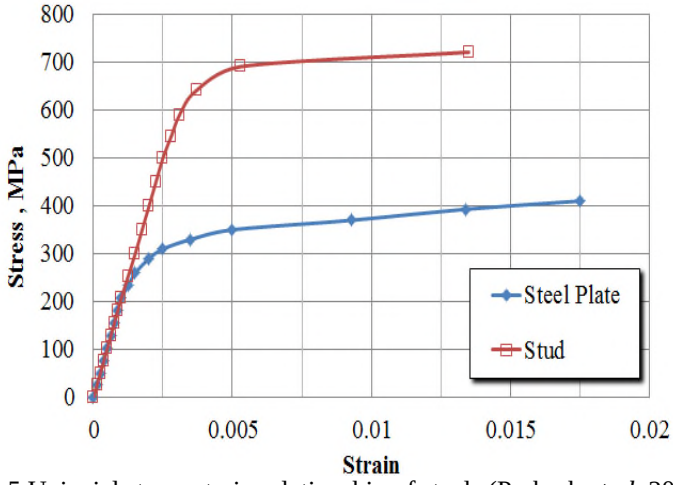

Fig. 5 Uniaxial stress-strain relationship of steels (Prakash *et al*. 2011)

assumed to comply with the von Mises failure criteria. The stress-strain relationship of the steel plate and the stud is shown in Fig. 5 based on the research by Prakash *et al*. (2011). The yielding strength and the tensile strength of the steel plate were 240 MPa and 400 MPa, respectively, while the yielding strength and tensile strength of the stud was 550 MPa and 710 MPa, respectively.

2.4 Boundary condition and analysis method

As shown in Fig. 6, to analyze SC walls subjected to in-plane cyclic loads, first, the boundary conditions of full restraints were applied in the lower part of the wall. In addition, the vertical displacement of the lateral direction was repeatedly loaded in the upper part of the wall. Fig. 6 shows a displacement history applied for each cyclic load. To generate it, seven cyclic loads up to maximum ± 6 mm were applied.

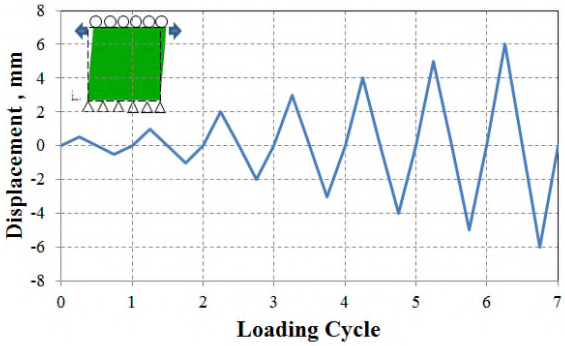

Fig. 6 Displacement history for numerical analyses

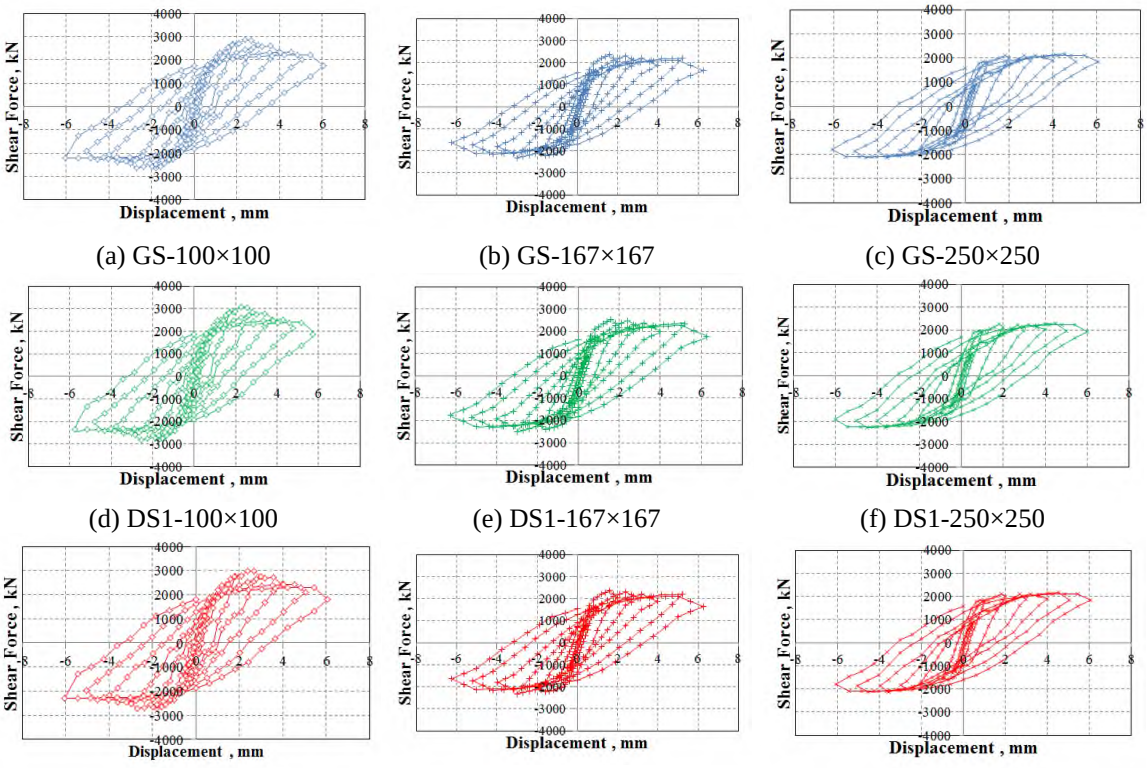

(a) GS-100×100 (b) GS-167×167 (c) GS-250×250

(d) DS1-100×100 (e) DS1-167×167 (f) DS1-250×250

(g) DS2-100×100 (h) DS2-167×167 (i) DS2-250×250

Fig. 7 Hysteresis curves from FE results

3. Analysis results and evaluation

3.1 Relationship between load and displacement

In-plane cyclic shear force was repeatedly applied to the wall, referring to the shear yielding strain and the existing experimental results of the steel plate and increasing gradually from level

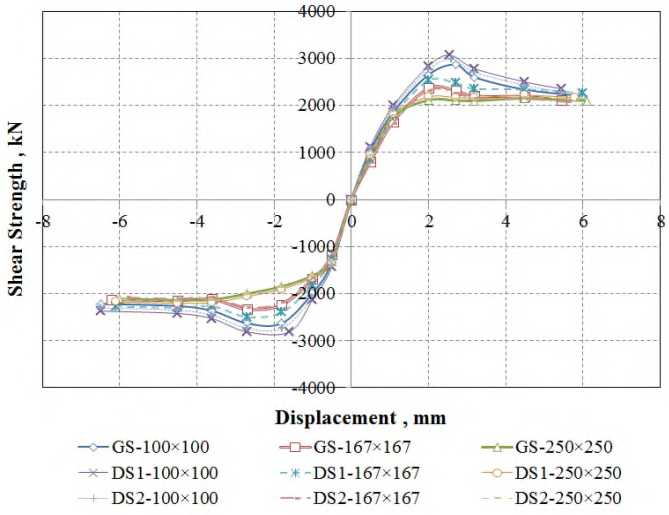

Fig. 8 Comparative P vs δ skeleton curves from numerical analyses

0.5 times of the displacement based on the maximum displacement of ±6 mm. The average displacement and reaction force at the upper and lower portions, respectively, of the wall were investigated. Fig. 7 shows the load-displacement hysteresis curves for each case. In addition, Fig. 8 shows the skeleton curves representing the relationship between the maximum shear force within each repeat history and the corresponding displacement.

For a case of 100 mm stud spacing in accordance with the provision of KEPIC SNG (2010) showed higher maximum shear strength than other stud distances. For the type of studs, when the distance is 100 mm, the shear strength of advanced studs (DS1 and DS2) was approximately 4~6% higher than GS. However, for other stud distances, the strengths exhibited slightly higher or similar levels than GS.

Table 3 shows the results summarized initial stiffness (K_I), ultimate strength (V_u), displacement corresponding at the ultimate strength (δ_u), yielding strength (V_Y), and yielding displacement (δ_Y) for repeated shear forces. For SC structures, unlike general steel, because the yielding point is not clear, 0.8 times the ultimate strength (V_u) was defined as the yielding strength (V_Y) with reference to the research of Elmenshawi and Brown (2010), and the corresponding displacement was determined as the yielding displacement.

Initial stiffness defined as the tangential stiffness at the initial cyclic load was higher since the synthesis is perfect between steel plate and concrete, the more narrow the spacing of studs. And, the case of studs having inclined members showed higher values. In the case of stud spacing 100mm in which the synthesis condition between steel plate and concrete is excellent, concrete was gradually damaged and completely destroyed after the fourth period. When the spacing of studs is gradually increased, however, the synthetic state was incompletely changed and it was confirmed that, at the early period, the concrete is completely damaged.

3.2 Damping ratio with decrease of the stiffness ratio

In order to evaluate the fracture pattern of the structure for repeated lateral loads such as

Table 3 Result summary of FE analyses

Model No.	Initial stiffness	Ultimate strength	Displacement		Yield strength
			at V_u	at V_y	
	K_I, kN/mm	V_u, kN	δ_u, mm	δ_y, mm	V_y, kN
GS-100×100	2510	2869	2.71	1.62	2295
GS-167×167	2410	2366	2.11	1.11	1893
GS-250×250	2386	2151	2.01	1.09	1721
DS1-100×100	2613	3069	2.55	1.52	2455
DS1-167×167	2501	2531	2.10	1.13	2025
DS1-250×250	2411	2216	2.01	1.10	1773
DS2-100×100	2607	2983	2.61	1.60	2386
DS2-167×167	2415	2318	2.08	1.14	1854
DS2-250×250	2399	2173	2.03	1.01	1738

earthquakes etc., a complex motion equation shall solve. However, it is not easy. Accordingly, the average stiffness decrease of the structure and equivalent viscous damping ratio were evaluated from load-displacement hysteresis curves as shown in Fig. 9. For actual structures, the average stiffness (K_a, Eq. (4)) by repeated loading decreases and the damping ratio increases while consuming the energy due to external forces.

$$K_a = \frac{P_m}{\delta_m}, \text{ kN/mm} \tag{4}$$

Where, K_a is the average stiffness at each period, P_m is the average maximum load at each cycle, and δ_m is the average maximum displacement. For single degree of freedom system structures, when the repeated lateral load acting as an external force is expressed in $P(t)=P_0\sin\omega t$, the energy dissipated by viscous damping (E_D) can be expressed as Eq. (5). This, as shown in Fig. 9, is equal to the area of load-displacement hysteresis curves by harmonic loads (Lee *et al*. 2007, Cho *et al*. 2013).

$$E_D = \int f_D \cdot d\delta = \int_0^{\frac{2\pi}{\omega}} \left(c\frac{d\delta}{dt} \right) \frac{d\delta}{dt} dt = \int_0^{\frac{2\pi}{\omega}} c\left(\frac{d\delta}{dt} \right)^2 dt, \text{ kN·mm} \tag{5}$$

Where, E_D is the dissipated energy, f_D is the external load, δ is the displacement, c is the damping factor, ω is the damping natural frequency of vibration, and t is the time. In addition, the strain energy of the structure (E_S) is the same as the Eq. (6) and the strain energy can represent by an approximate strain energy (E_{S0}) of Eq. (7), and this is equal to the area of the portion indicated by hatching in Fig. 8 (Lee *et al*. 2007, Cho *et al*. 2013).

$$E_S = \int f_S \cdot d\delta = \int_0^{\frac{2\pi}{\omega}} \left(K_a \cdot \delta \right) \frac{d\delta}{dt} dt, \text{ kN·mm} \tag{6}$$

$$E_{S0} = \frac{1}{2} K_a \delta_m^{\,2}, \text{ kN·mm} \tag{7}$$

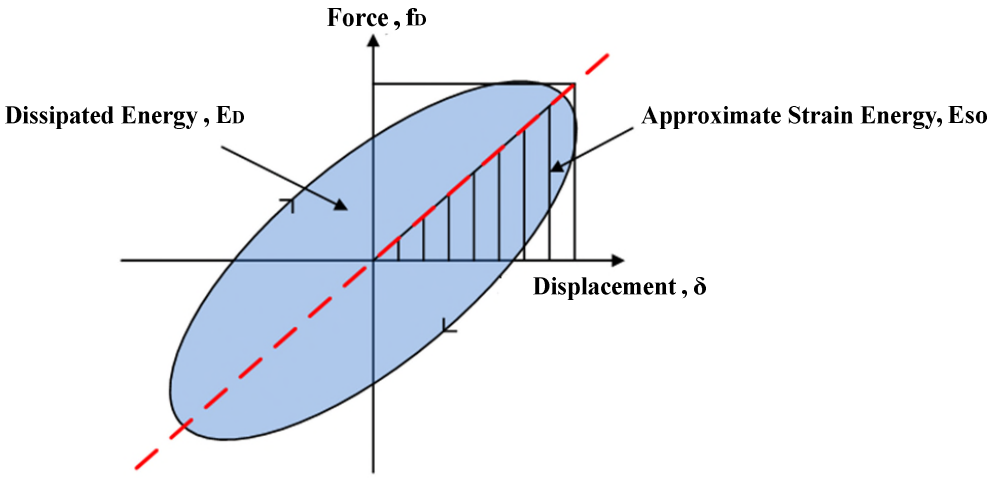

Fig. 9 Hysteresis curve for viscous damping (Cho *et al*. 2013)

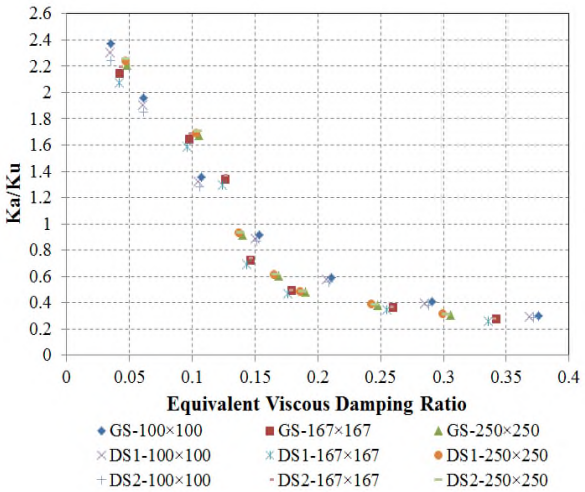

Fig. 10 Stiffness ratio vs equivalent viscous damping ratio

Where, E_S is the strain energy, E_{S0} is the approximate strain energy, and f_s is the internal force. From the relationship between dissipated energy and strain energy due to the damping of the structure, the equivalent viscous damping ratio at the ith period (ξ_{ei}) can be obtained from Eq. (8) (Lee *et al*. 2007, Cho *et al*. 2013).

$$\xi_{ei} = \frac{1}{4\pi}\frac{E_{Di}}{E_{S_0 i}} \tag{8}$$

Fig. 10 shows the relationship between the stiffness ratio and equivalent viscous damping ratio. Where the stiffness ratio (K_a/K_u) was defined as a value obtained by dividing the average stiffness of each period (K_a) to the stiffness at the ultimate strength (K_u). At the first period, equivalent

viscous damping ratio was counted as 2.5 to 4.7 percent level. This was a similar level with damping ratio obtained through the free vibration tests applied lower level than the ultimate strength (Lee and Kim 2010).

Cho *et al*. (2013), through repeated load tests on small-scaled SC specimens performed in the laboratory, obtained equivalent viscous damping ratio of approximately 6% at the K_a/K_u level of 2.0 (i.e., half of the ultimate strength). Where, analysis results also showed a similar level. In addition, the studies of Cho *et al*. (2013) reported that equivalent viscous damping ratio is approximately 10% at the K_a/K_u level of 1.15~1.25 (i.e., 80% of the ultimate strength). However, this study performed FEA showed the damping ratio of approximately 11~13%. KEPIC SNG defines that the damping ratio at the level of stability earthquake is 6% since SC structures have a little cracks than RC structures. However, from analysis results, it was confirmed that the smaller the stiffness ratio, the damping ratio increased due to the damage involving the cracking in concrete.

3.3 Cumulative dissipation energy

Generally, it was noted that the greater the energy dissipation capacity, aseismic performance is to be excellent. Dissipation energy is the energy accepted while the structure maintaining the internal force and it can be calculated as the sum of areas surrounded by the load-displacement hysteresis curves. Accordingly, in this paper, the dissipation energy at each cycle was calculated through these curves and the cumulative dissipated energy was estimated by accumulating the values.

Fig. 11 shows the cumulative dissipated energy at each period of SC walls subjected to repeated cyclic loads. Based on the seventh period, the cumulative dissipated energy of GS 167mm and 250mm compared to GS 100mm spacing were 85% and 82% level, respectively. This

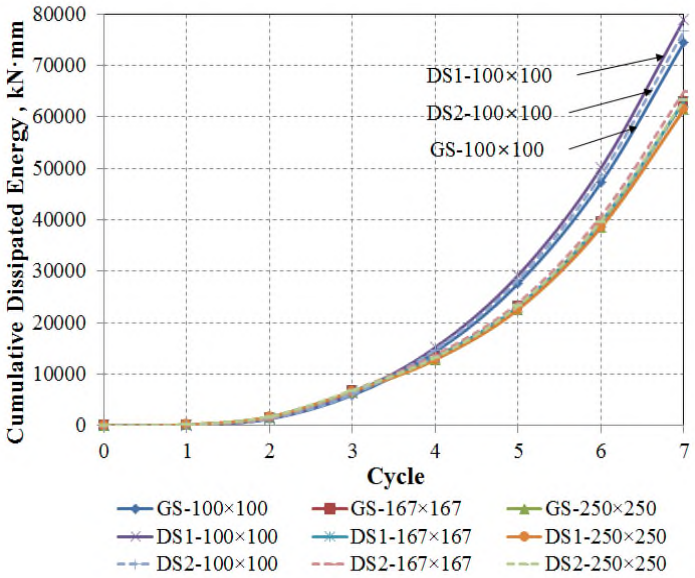

Fig. 11 Cumulative dissipated energy from FE analyses

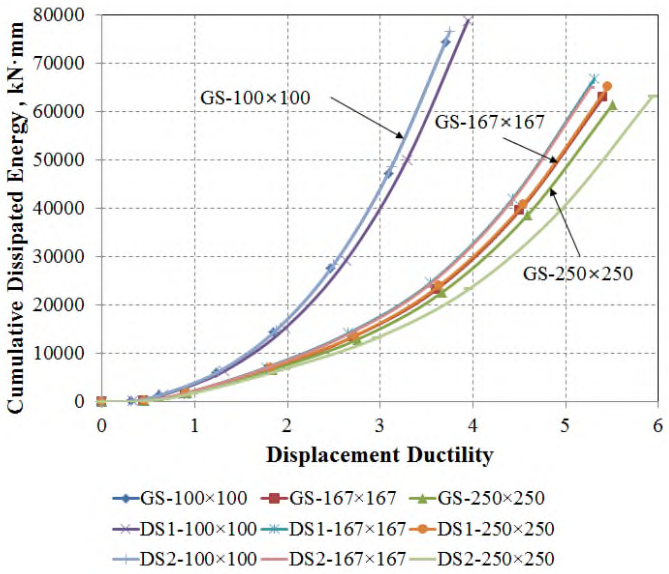

Fig. 12 Cumulative dissipated energy-displacement ductility relationship

means, when the synthesis between steel plate and concrete are incomplete, the seismic performance was decreased since the spacing between the studs is too large. For DS1 consisted of two inclined studs and one parallel stud, the cumulative dissipated energy was as high as approximately 7% compared to GS. In addition, for DS2 consisted of two inclined studs, the cumulative dissipated energy was as high as approximately 4%.

3.4 Cumulative dissipation energy and displacement ductility

When the ductility of materials is greater, it can absorb considerable energy prior to destruction. Due to this reason, the ductility as an indicator to evaluate the performance of the structure subjected to earthquake as well as the cumulative dissipated energy is used.

As shown in Eq. (9), the indicator representing the ductility effect resistant to the inelastic deformation can represent as the value divided by maximum displacement (δ_{max}) to yielding displacement (δ_Y) for load-displacement hysteresis curves. This is called displacement ductility or ductility factor (DF).

$$DF = \frac{\delta_{max}}{\delta_Y} \tag{9}$$

Fig. 12 shows the relationship between cumulative dissipation energy and displacement ductility with spacing and shape of studs. When they have the same cumulative energy dissipation capability, it showed excellent ductility depending on the spacing apart of studs. This is because the yielding happened at the displacement and load stage of the early states than normal case due to incomplete synthesis between steel plate and concrete. In addition, when the stud spacing is 100 mm, the ductility of DS1 appeared to be slightly superior and DS2 showed a very similar level with GS. However, for more stud distances, the trend did not become apparent. Accordingly, it is

noted that, when the connection between steel plate and concrete is poor, to evaluate the seismic performance from the relationship between the cumulative dissipated energy and ductility is not reasonable.

4. Conclusions

This research has analytically examined the effect of the shape and spacing of studs used as shear connectors in NPPs on the performance of SC walls subjected to cyclic shear loads and the following results were obtained.

- The skeleton curves from the load-displacement hysteresis obtained through the analyses for cyclic loading were obtained. From this, ultimate strength, yielding strength, and their corresponding displacements were obtained. The narrower the gap between the studs, ultimate strength and yielding strength showed significant and the strengths of developed studs having inclined members than general stud were larger.
- The damping ratio was calculated from load-displacement hysteresis curves, as a result of comparing them with the stiffness, it was confirmed that the damping ratio increases depending on the stiffness ratio is reduced. It showed damping ratio of approximately 6% in half of the ultimate strength and damping ratio of approximately 11~13% at 80% of the ultimate strength.
- Cumulative dissipation energy was obtained by accumulation them after calculating the dissipated energy from the load-displacement hysteresis curve. The results compared each case showed that cumulative damage energy appears significant and the seismic performance is more excellent as the distance between the studs decreases. In the case of DS1 and DS2, compared with GS, the energy was great approximately 7% and 4%, respectively.
- When the spacing of studs increases, the walls yield in the low level of loads than normal case due to incomplete synthesis. In this case, to evaluate the seismic performance from the relationship between cumulative dissipated energy and ductility does not look to be reasonable.

Acknowledgments

The research described in this paper was financially supported by the Basic Science Research Program of the National Research Foundation of Korea (NRF-2014R1A1A2056504).

References

ACI Committee 318-11 (2011), Building Code Requirements for Structural Concrete (ACI 318-11) and Commentary (ACI 318R-11), Farmington Hills (MI): American Concrete Institute.

Carreira, D.J. and Chu, K.H. (1985), "Stress-strain relationship for plain concrete in compression", *ACI J.*, **82**(6), 797-804.

Cho, S.G., So, G.H. and Park, W.K. (2013), "Investigation of damping ratio of steel plate concrete shear wall by lateral loading test&impact test", *J. Earthq. Eng. Soc. Korea*, **17**(2), 79-88. (in Korean)

Cho, S.G., Lim, J.S., Jeong, Y.D., Yi, S.T. and Han, S.M. (2014), "Analytical study for performance improvement of studs for steel plate concrete walls subjected to bending moment", *Eng. Struct.* (submitted)

Cho, S.G. and Yi, S.T. (2014), "Shape and arrangement of developed studs in a steel plate concrete wall

subjected to shear force and axial force", *P. I. Civil Eng.-Str. B.* (submitted)
Elmenshawi, A. and Brown, T. (2010), "Hysteretic energy and damping capacity of flexural elements constructed with different concrete strengths", *Eng. Struct.*, **32**(1), 297-305.
Epackachi, S., Nguyen, N., Kurt, E., Whittaker, A. and Varma, A. (2015), "In-plane seismic behavior of rectangular steel-plate composite wall piers", *J. Struct. Eng.*, **141**(7), 04014176.
Evans, R.H. and Marathe, M.S. (1967), "Microcracking and stress-strain curves for concrete in tension", *Mater. Struct.*, **1**(1), 61-64.
Jankowiak, T. and Lodygowski, T. (2005), "Identification of parameters of concrete damage plasticity constitutive model", *Foundation of Civil and Environmental Engineering*, No. 6, Poznan university of technology, Poland.
Korea Concrete Institute (KCI) (2012), *The Korean Concrete Structure Design Code*, Korea Concrete Institute. (in Korean)
Korea Electric Association (KEA) (2010), *Nuclear Safety Related Structures: Steel-Plate Concrete Structure*, Korea Electric Association. (in Korean)
Lee, K.H., Kim, H.C., Hong, W.K. and Lee, Y.H. (2007), "Capacity of concrete filled carbon tube columns based on the comparison of ductility and energy dissipation capacity", *J. Earthq. Eng. Soc. Korea*, **11**(1), 29-35. (in Korean)
Lee, S.J. and Kim, W.K. (2010), "Damping ratios for seismic design of SC structures", *J. Korean Soc. Steel Constr.*, **22**(5), 487-496. (in Korean)
Lim, J.S., Jeong, Y.D. and Yi, S.T. (2015), "Analytical study for performance evaluation of studs for steel plate concrete walls subjected to cyclic loads", *J. Korea Inst. Struct. Maint. Insp.*, **19**(4), 35-42.
Ozaki, M., Akita, S., Oosuga, H., Nakayama, T. and Adachi, N. (2004), "Study on steel plate reinforced concrete panels subjected to cyclic in-plane shear", *Nucl. Eng. Des.*, **228**(1), 225-244.
Prakash, A., Anandavalli, N., Madheswaran, C.K., Rajasankar, J. and Lakshmanan, N. (2011), "Three dimensional FE model of stud connected steel-concrete composite girders subjected to monotonic loading", *Int. J. Mech. Appl.*, **1**(1), 1-11.
Ren, W., Sneed, L.H., Gai, Y. and Kang, X. (2015a), "Test results and nonlinear analysis of RC T-beams strengthened by bonded steel plates", *Int. J. Concrete Struct. Mater.*, **9**(2), 133-143.
Ren, W., Sneed, L.H., Yang, Y. and He, R. (2015b), "Numerical simulation of prestressed precast concrete bridge deck panels using damage plasticity model", *Int. J. Concrete Struct. Mater.*, **9**(1), 45-54.
Shahidul Islam, S.M. and Khennane, A. (2013), "Computer aided design of RC structures", *Int. J. Concrete Struct. Mater.*, **7**(2), 127-133.
Vecchio, F.J. and McQuade, I. (2011), "Towards improved modeling of steel-concrete composite wall elements", *Nucl. Eng. Des.*, **241**(8), 2629-2642.